Vibrational Structure of Titanium Silicate Catalysts. A Spectroscopic and Theoretical Study

Gabriele Ricchiardi,*,† Alessandro Damin,† Silvia Bordiga,† Carlo Lamberti,†,‡ Guido Spanò,§ Franco Rivetti,§ and Adriano Zecchina†

Contribution from the Dipartimento di Chimica, IFM Università di Torino, Via P. Giuria 7, 10125 Turin, Italy, INFM Unità di Torino Università, Turin, Italy, and EniChem S.p.A. Centro Ricerche, Novara Istituto G. Donegani, Via G. Fauser 4, I-28100 Novara, Italy

Received March 6, 2001. Revised Manuscript Received May 30, 2001

Abstract: A thorough analysis of the vibrational features of the titanium silicalite-1 (TS-1) catalyst is presented, based on quantitative IR measurements, Raman and resonant Raman experiments, quantitative XANES, and quantum chemical calculations on cluster and periodic models. The linear correlation of the intensity of the IR and Raman bands located at 960 and 1125 cm^{-1} and the XANES peak at 4967 eV with the amount of tetrahedral Ti are quantitatively demonstrated. Raman and resonant Raman spectra of silicalite and TS-1 with variable Ti content are presented, showing main features at 960 and 1125 cm^{-1} associated with titanium insertion into the zeolite framework. The enhancement of the intensity of the 1125 cm^{-1} feature and the invariance of the 960 cm^{-1} feature in UV−Raman experiments, are discussed in terms of resonant Raman selection rules. Quantum chemical calculations on cluster models $Si[OSi(OH)_3]_4$ and $Ti[OSi(OH)_3]_4$ at the B3LYP/6-31G(d) level of theory provide the basis for the assignment of the main vibrational contributions and for the understanding of Raman enhancement. The resonance-enhanced 1125 cm^{-1} mode is unambiguously associated with a totally symmetric vibration of the TiO_4 tetrahedron, achieved through in-phase antisymmetric stretching of the four connected Ti−O−Si bridges. This vibration can also be described as a totally symmetric stretching of the four Si−O bonds pointing toward Ti. The resonance enhancement of this feature is explained in terms of the electronic structure of the Ti-containing moiety. Asymmetric stretching modes of TO_4 units show distinct behavior when (i) T is occupied by Si as in perfect silicalite, (ii) T is occupied by Ti as in TS-1, or (iii) the oxygen atom belongs to an OH group, such as in terminal tetrahedra of cluster models and in real defective zeolites. Asymmetric SiO_4 and TiO_4 stretching modes appear above and below 1000 cm^{-1}, respectively, when they are achieved through antisymmetric stretching of the T−O−Si bridges, and around 800 cm^{-1} (in both SiO_4 and TiO_4) when they involve symmetric stretching of the T−O−Si units. In purely siliceous models, the transparency gap between the main peaks at 800 and 1100 cm^{-1} contains only vibrational features associated with terminal Si−OH groups, while in Ti−containing models it contains also the above-mentioned asymmetric TiO_4 modes, which in turn are strongly coupled with Si−OH stretching modes. Calculations on periodic models of silicalite and TS-1 free of OH groups using the QMPOT embedding method correctly reproduce the transparency gap of silicalite and the appearance of asymmetric TiO_4 vibrations at 960 cm^{-1} in TS-1. Finally, we demonstrate, for the first time, that the distortion of the tetrahedral symmetry around Ti caused by water adsorption quenches the UV−Raman enhancement of the 1125 cm^{-1} band.

1. Introduction

Titanium silicalite-1 (TS-1) is a synthetic zeolite[1] in which a small number of Ti atoms substitute tetrahedral Si atoms in a purely siliceous framework with the MFI structure.[2] It is an active and selective catalyst in a number of low-temperature oxidation reactions with aqueous H_2O_2 as the oxidant.[3−9] For this reason, it has been one of the most studied materials in heterogeneous catalysis in past years. Although the long-range structure of the material is well-known,[10−13] the structure of the active site is not clear. This structure can be discussed at

* To whom correspondence should be addressed: Telephone: +39011-6707845. Fax: +39011-6707855. E-mail: ricchiardi@ch.unito.it.

† Dipartimento di Chimica IFM, Università di Torino.

‡ INFM Unità di Torino.

§ Instituto G. Donegani Novara.

(1) Taramasso, M.; Perego, G.; Notari, B. U.S. Patent No. 4410501, 1983.

(2) Meier, W. M.; Olson, D. H.; Baerlocher, Ch. *Atlas of Zeolite Structure Types*; Elsevier: London, 1996. Thomas, J. M.; Bell, R. G.; Catlow, C. R. A. In *Handbook of Heterogeneous Catalysis*; Ertl, G., Knözinger, H., Weitkamp, J., Eds.; VCH: Weinheim, Germany, 1997; pp 286−310.

(3) Clerici, G. M. *Appl. Catal.* **1991**, *68*, 249.

(4) Clerici, G. M.; Bellussi, G.; Romano, U. *J. Catal.* **1991**, *129*, 159.

(5) Bellussi, G.; Carati, A.; Clerici, G. M.; Maddinelli, G.; Millini, R. *J. Catal.* **1992**, *133*, 220.

(6) Notari, B. *Adv. Catal.* **1996**, *41*, 253, and references cited therein.

(7) Roffia, P.; Leofanti, G.; Cesana, A.; Mantegazza, M. A.; Padovan, M.; Petrini, G.; Tonti, S.; Gervasutti, P. *Stud. Surf. Sci. Catal.* **1990**, *55*, 543.

(8) Mantegazza, M. A.; Leofanti, G.; Petrini, G.; Padovan, M.; Zecchina, A.; Bordiga, S. *Stud. Surf. Sci. Catal.* **1994**, *82*, 541.

(9) Mantegazza, M. A.; Petrini, G.; Spanò, G.; Bagatin, R.; Rivetti, F. *J. Mol. Catal. A* **1999**, *146*, 223.

(10) Millini, R.; Previdi Massara, E.; Perego, G.; Bellussi, G. *J. Catal.* **1992**, *137*, 497.

(11) Lamberti, C.; Bordiga, S.; Zecchina, A.; Carati, A.; Fitch, A. N.; Artioli, G.; Petrini, G.; Salvalaggio, M.; Marra, G. L. *J. Catal.* **1999**, *183*, 222.

(12) Marra, G. L.; Artioli, G.; Fitch, A. N.; Milanesio, M.; Lamberti, C. *Microporous Mesoporous Mater.* **2000**, *40*, 85.

(13) Lamberti, C.; Bordiga, S.; Zecchina, A.; Artioli, G.; Marra, G. L.; Spanò, G., *J. Am. Chem. Soc.* **2001**, *121*, 2204.

10.1021/ja010607v CCC: $20.00
Published on Web 10/30/2001

different levels of detail: titanium coordination and bond distances (regardless of its position in the framework), possible localization of Ti on specific framework sites, coordination under synthesis and reaction conditions (e.g. with adsorbates), occurrence and structure of extraframework Ti species, mechanism of Ti extraction, or insertion from or in the framework. All these aspects are important in catalysis studies, because it is not known which species—whether the bare framework tetrahedral or some kind of complexed or modified structure—are catalytically active.

Several experimental[10−37] and computational[14,38−47] results demonstrate that the substitution of Si by Ti is isomorphous in well-prepared samples, and it is generally believed that the distribution of Ti over the available framework sites is at least partially disordered.[48] A variety of techniques have been developed, able to detect and discriminate tetracoordinated framework titanium from extraframework titanium atoms with higher coordination. Among these we cite vibrational spectroscopies (both IR and Raman),[14−24] UV−vis,[19,23,24,29,30] EXAFS,[24−34] and XANES,[24−26,28,30,31,33−35] spectroscopies and powder diffraction experiments (using both X-rays and neutrons).[10−13] The first two methods in particular, due to their ease of use, have become standard analysis techniques for catalysts containing titanium. The infrared feature which is more clearly associated with the presence of tetrahedrally coordinated framework Ti is a relatively strong absorption appearing, in dehydrated samples, at 960 cm^{-1}.

A qualitative correlation between the intensity of the infrared band at 960 cm^{-1} and the titanium content has been observed since the first synthesis of TS-1. Indeed, the occurrence of that band is one of the distinctive features of the material cited in the original patent.[1] However, no quantitative correlation has been published to date. The assignment and quantification of this band are complicated by the fact that hydroxyls and Si−O− groups of defect sites absorb in the same range.[17,49−51] Recently, the attribution of that band has been put into question on the basis of UV−resonant Raman experiments.[22] Since some of us were involved in the elaboration of the previously accepted model for the explanation of the 960 cm^{-1} band,[14−18,24] and because of the practical importance of the validation of IR

(14) Tozzola, G.; Mantegazza, M. A.; Ranghino, G.; Petrini, G.; Bordiga, S.; Ricchiardi, G.; Lamberti, C.; Zulian, R.; Zecchina, A. *J. Catal.* **1998**, *179*, 64.

(15) Boccuti, M. R.; Rao, K. M.; Zecchina, A.; Leofanti, G.; Petrini, G. *Stud. Surf. Sci. Catal.* **1989**, *48*, 133.

(16) Zecchina, A.; Spoto, G.; Bordiga, S.; Padovan, M.; Leofanti, G. *Stud. Surf. Sci. Catal.* **1991**, *65*, 671.

(17) Scarano, D.; Zecchina, A.; Bordiga, S.; Geobaldo, F.; Spoto, G.; Petrini, G.; Leofanti, G.; Padovan, M.; Tozzola, G. *J. Chem. Soc., Faraday Trans.* **1993**, *89*, 4123.

(18) Deo, G.; Turek, A. M.; Wachs, I. E.; Huybrechts, D. R. C.; Jacobs, P. A. *Zeolites* **1993**, *13*, 365.

(19) Zecchina, A.; Spoto, G.; Bordiga, S.; Ferrero, A.; Petrini, G.; Padovan, M.; Leofanti, G. *Stud. Surf. Sci. Catal.* **1991**, *69*, 251.

(20) Huybrechts, D. R.; Buskens, P. L.; Jacobs, P. A. *J. Mol. Catal.* **1992**, *71*, 129.

(21) van der Pol, A. J. H. P.; van Hooff, J. H. C. *Appl. Catal. A* **1992**, *92*, 93.

(22) Li, C.; Xiong, G.; Xin, Q.; Liu, J.; Ying, P.; Feng, Z.; Li, J.; Yang, W.; Wang, Y.; Wang, G.; Liu, X.; Lin, M.; Wang, X.; Min, E. *Angew. Chem., Int. Ed.* **1999**, *38*, 2220.

(23) Blasco, T.; Camblor, M.; Corma, A.; Pérez-Parriente, J. *J. Am. Chem. Soc.* **1993**, *115*, 11806.

(24) Bordiga, S.; Coluccia, S.; Lamberti, C.; Marchese, L.; Zecchina, A.; Boscherini, F.; Buffa, F.; Genoni, F.; Leofanti, G.; Petrini, G.; Vlaic, G. *J. Phys. Chem.* **1994**, *98*, 4125.

(25) Bordiga, S.; Boscherini, F.; Coluccia, S.; Genoni, F.; Lamberti, C.; Leofanti, G.; Marchese, L.; Petrini, G.; Vlaic, G.; Zecchina, A. *Catal. Lett.* **1994**, *26*, 195.

(26) Pei, S.; Zajac, G. W.; Kaduk, J. A.; Faber, J.; Boyanov, B. I.; Duck, D.; Fazzini, D.; Morrison, T. I.; Yang, D. S. *Catal. Lett.* **1993**, *21*, 333.

(27) Le Noc, L.; Trong On, D.; Solomykina, S.; Echchahed, B.; Bél, F.; Cartier dit Moulin, C.; Bonneviot, L. *Stud. Surf. Sci. Catal.* **1996**, *101*, 611.

(28) Zecchina, A.; Bordiga, S.; Lamberti, C.; Ricchiardi, G.; Scarano, D.; Petrini, G.; Leofanti, G.; Mantegazza, M. *Catal. Today* **1996**, *32*, 97.

(29) Lamberti, C.; Bordiga, S.; Arduino, D.; Zecchina, A.; Geobaldo, F.; Spanò, G.; Genoni, F.; Petrini, G.; Carati, A.; Villain, F.; Vlaic, G. *J. Phys. Chem. B* **1998**, *102*, 6382.

(30) Trong On, D.; Le Noc, L.; Bonneviot, L. *Chem. Commun.* **1996**, 299.

(31) Lamberti, C.; Turnes Palomino, G.; Bordiga, S.; Arduino, D.; Zecchina, A.; Vlaic, G. *Jpn. J. Appl. Phys.* **1999**, *38−1*, 55.

(32) Gleeson, D.; Sankar, G.; Catlow, C. R. A.; Thomas, J. M.; Spanò, G.; Bordiga, S.; Zecchina, A.; Lamberti, C. *Phys. Chem. Chem. Phys.* **2000**, *2*, 4812.

(33) Bolis, V.; Bordiga, S.; Lamberti, C.; Zecchina, A.; Petrini, G.; Rivetti, F.; Spanò, G. *Langmuir* **1999**, *155*, 753.

(34) Bolis, V.; Bordiga, S.; Lamberti, C.; Zecchina, A.; Petrini, G.; Rivetti, F.; Spanò, G. *Microporous, Mesoporous Mater.* **1999**, *30*, 67.

(35) Bordiga, S.; Geobaldo, F.; Lamberti, C.; Zecchina, A.; Boscherini, F.; Genoni, F.; Leofanti, G.; Petrini, G.; Padovan, M.; Geremia, S.; Vlaic, G. *Nucl. Instrum. Meth. Phys. Res., Sect. B* **1995**, *97*, 23.

(36) Millini, R.; Perego, G. *Gazz. Chim. Ital.* **1996**, *126*, 133.

(37) Vayssilov, G. N. *Catal. Rev.—Sci. Eng.* **1997**, *39*, 209.

(38) Jentys, A.; Catlow, C. R. A. *Catal. Lett.* **1993**, *22*, 251.

(39) Millini, R.; Perego, G.; Seiti, K. *Stud. Surf. Sci. Catal.* **1994**, *84*, 2123.

(40) de Man, A. J. M.; Sauer, J. *J. Phys. Chem.* **1996**, *100*, 5025.

(41) Oumi, Y.; Matsuba, K.; Kubo, M.; Inui, T.; Miyamoto, A. *Microporous Mater.* **1995**, *4*, 53.

(42) Smirnov, K. S.; van de Graaf, B. *Microporous Mater.* **1996**, *7*, 133.

(43) Njo, S. L.; van Koningsveld, H.; van de Graaf, B. *J. Phys. Chem. B* **1997**, *101*, 10065.

(44) Sinclair, P. E.; Sankar, G.; Catlow, C. R. A.; Thomas, J. M.; Maschmeyer, T. *J. Phys. Chem. B* **1997**, *101*, 4237.

(45) Zicovich-Wilson, C. M.; Dovesi, R.; Corma, A. *J. Phys. Chem. B* **1999**, *103*, 988.

(46) Sinclair, P. E.; Catlow, C. R. A. *J. Phys. Chem. B* **1999**, *103*, 1084.

(47) Ricchiardi, G.; de Man, A.; Sauer, J. *Phys. Chem. Chem. Phys.* **2000**, *2*, 2195.

(48) In this regard, it should be noticed that, due to the small amount of Ti atoms that can be isomorphically inserted in the MFI framework, most of the studies concerning Ti partitioning (among the 12 crystallographically unequivalent T sites) are based on computational approaches. The first theoretical contributions to this debate came from Jentys and Catlow and from Millini et al. Both groups suggest a random distribution of Ti atoms. Oumi et al. reported a molecular dynamics (MD) approach claiming T8 as the preferential substitution site. In a subsequent MD work Smirnov and van de Graaf were not able to reproduce the results of Oumi et al. More recently, Njo et al. reported a study based on combined Metropolis Monte Carlo and molecular dynamics claiming T2 and T12 as preferential sites for Ti partitioning. Finally, Ricchiardi underlines how hydration (i.e. the presence of water molecules in the coordination sphere of Ti) must be considered when discussing Ti substitution in the framework sites on an energetic ground. As far as experimental works are concerned, both ^{49}Ti and ^{47}Ti NMR studies [Berger, S.; Bock, W.; Marth, C.; Raguse, B.; Reetz, M. *Magn. Reson. Chem.* **1990**, *28*, 559. Lopea, A.; Tuilier, M.; Guth, J.; Delmotte, L.; Popa, J. *Solid State Chem.* **1993** *102*, 480] have been attempted, but difficulties have been found due to the large quadrupolar moment of both nuclei. Adsorption microcalorimetry results, using NH_3 as probe, found that the heat of adsorption at the Ti(IV) sites was typical of heterogeneous surfaces. This result discarded the presence of one single preferred substituted site, and the authors concluded that Ti should be either randomly distributed or preferentially located in several preferential sites. Even the use of the intense X-ray flux emitted by synchrotron has not permitted the unambiguous detection of preferential substitution sites by XRD methods, and only ad hoc measurements, performed at 170 K, gave very weak evidence that Ti has a preferential tendency to occupy sites T10 and T11. Very recently, a neutron diffraction study indicated that the most populated sites are T6, T7, and T11, with weaker evidence for T10.

(49) Zecchina, A.; Bordiga, S.; Spoto, G.; Marchese, L.; Petrini, G.; Leofanti, G.; Padovan, M.; *J. Phys. Chem.* **1992**, *96*, 4985. Zecchina, A.; Bordiga, S.; Spoto, G.; Marchese, L.; Petrini, G.; Leofanti, G.; Padovan, M. *J. Phys. Chem.* **1992**, *96*, 4991. Zecchina, A.; Bordiga, S.; Spoto, G.; Marchese, L.; Petrini, G.; Leofanti, G.; Padovan, M.; Otero Areàn, C. *J. Chem. Soc., Faraday Trans.* **1992,** *88*, 2959. Marra, G. L.; Tozzola, G.; Leofanti, G.; Padovan, M.; Petrini, G.; Genoni, F.; Venturelli, B.; Zecchina, A.; Bordiga, S.; Ricchiardi, G. *Stud. Surf. Sci. Catal.* **1994**, *84*, 559.

(50) Camblor, M. A.; Corma, A.; Perez-Pariente, J. *J. Chem. Soc., Chem. Commun.* **1993**, 557.

(51) Bordiga, S.; Ugliengo, P.; Damin, A.; Lamberti, C.; Spoto, G.; Zecchina, A.; Spanò, G.; Buzzoni, R.; Dalloro, L.; Rivetti, F. *Top. Catal.* **2001**, *15*, 43. Bordiga, S.; Roggero, I.; Ugliengo, P.; Zecchina, A.; Bolis, V.; Artioli, G.; Buzzoni, R.; Marra, G. L.; Rivetti, F.; Spanò, G.; Lamberti, C. *J. Chem. Soc., Dalton Trans.* **2000**, 3921.

spectroscopy as a screening tool for catalyst preparations, we have undertaken a thorough reexamination of the experiments and models proposed so far, whose results are exposed in this paper.

In the rest of this introduction we will first briefly review the models proposed to interpret the 960 cm^{-1} band and then introduce the recent Raman results from the literature and our own Raman investigations.

The earlier interpretation of the 960 cm^{-1} band[15] was based on the discussion of the modes of isolated SiO_4 tetrahedra as compared with tetrahedra neighboring with a TiO_4 unit. Assuming a higher ionicity of the Ti−O bond as compared with the Si−O one (later confirmed by quantum mechanical calculations), the Si−O stretching mode was expected to shift downward due to the interaction with the Ti cation ($Si-O^{\delta-}...Ti^{\delta+}$). On the basis of quantum mechanical calculations on cluster models, it was later proposed, by de Man and Sauer,[40] that the mode is a simple antisymmetric stretching of the Si−O−Ti bridge. Indeed the two assignments may be seen as coincident, because they describe the same physical mode by focusing on different "building units".[17,52] Smirnov and van de Graaf[42] calculated the vibrational spectra of a periodic model of TS-1 with molecular dynamics techniques. Their results support the localized Ti−O−Si nature of the 960 cm^{-1} vibration, and they also put into evidence that the Si−O and Ti−O bonds are not equivalent and that the Si−O stretching gives the greater contribution to the vibration, in substantial agreement with the previous assignment.[15,17]

From this point of view, the 960 cm^{-1} vibration is considered to be the collective vibration of four coupled Si−O oscillators arranged tetrahedrally, perturbed by the presence of the Ti atom, viewed as a structural impurity or defect. Another moiety with the same arrangement of Si−O bonds can be obtained by removing a Si atom from the lattice, as in the so-called hydrogarnet defect.[51] As already demonstrated for Ti, it is reasonable to suppose that also the presence of four OH groups perturbs the adjacent Si−O vibrations. According to this view, Camblor et al.[50] have concluded that the 960 cm^{-1} band is a Si−O− vibration in defects. However, the two assignments are not mutually exclusive because both defects could contribute to the presence of IR components in the same spectral range. In this work we will show that the vibrational features of framework Ti and of defect sites are distinct but strongly coupled.

Very recently, it has been proposed[22] that the 960 cm^{-1} band may be only a minor, secondary manifestation of the presence of Ti in the framework, the real fingerprint being a Raman active band at 1125 cm^{-1}, together with two less intense components at 490 and 530 cm^{-1}. The fact that the 960 cm^{-1} band is not enhanced by UV−resonance has been assumed by the authors of ref 22 to prove that the group responsible for it does not lie in the immediate vicinity of the Ti atom. We will confute this assumption in the following of this paper. The existence of a component at 1125 cm^{-1} in the Raman spectra of TS-1 correlated with the presence of Ti in the MFI framework had been already reported in 1993 by Scarano et al.[17] and by the group of Jacobs[18] using conventional Raman spectroscopy, but the discovery of its UV−Raman enhancement, reported in ref 22 for the first time, allows one to extract new important information on the vibrational properties of TS-1.

Scarano et al.[17] have also demonstrated that if other M heteroatoms are substituted in the MFI framework (M = Fe, Al, B), the corresponding peculiar IR bands appear to be only weakly shifted (up to 16 cm^{-1}) with respect to that found for TS-1. According to the pioneering attribution,[15] Scarano et al.[17] concluded that the 960 cm^{-1} band in TS-1, the 975 cm^{-1} band in defective silicalites, and other similar bands observed in other M-substituted MFI systems (in the 960−976 cm^{-1} range) are due to a stretching mode with prevailing Si−O character, slightly perturbed by the presence in the next T position of a M heteroatom (or a Si vacancy). In such a case the heteroatom plays the role of a "defect" in the perfect periodicity of the crystal, and thus its perturbation to the Si−O stretching is expected to be only slightly dependent on the nature of M. Recent UV−Raman experiments[53] show the presence of high-frequency modes in Fe−ZSM-5 at 1122, 1125, and 1175 cm^{-1}.

Coming back to TS-1, we shall demonstrate that the fact that the 1125 cm^{-1} mode is strongly enhanced by UV resonance, while for 960 cm^{-1} it is not, can be understood by considering the different selection rules which apply to resonant and normal Raman experiments. Once these rules are applied, relevant information on the nature of the corresponding modes will be obtained.

To help further reading we will briefly recall that resonant Raman spectroscopy is defined as a Raman experiment in which the exciting wavelength coincides with or is near to the wavelength of an electronic adsorption of the sample. This condition guarantees a high transfer of energy to the sample. Moreover, the use of a UV exciting source guarantees a relevant reduction of the fluorescence background. If the electronic absorption is due to a localized center, like a transition metal atom, excitation is also partially localized and the vibrational features of the immediate vicinity of the absorbing atom can be enhanced by several orders of magnitude, if they meet the appropriate enhancement selection rules. Two kinds of vibrations are enhanced: (a) totally symmetric vibrations with respect to the absorbing center and (b) vibrations along modes which cause the same molecular deformation induced by the electronic excitation.[54]

From all these considerations it is evident that careful comparison of the IR, Raman, and resonant-Raman spectra of TS-1 samples at increasing Ti loading (including a Ti-free silicalite sample), supported by quantum mechanical calculations on model compounds, is indispensable in giving information on the symmetry of the modes involving the Ti atom. This global approach will lead to the achievement of a deeper understanding of the vibrational features of TS-1.

2. Experimental Section

Four TS-1 samples with increasing Ti content have been synthesized in EniChem laboratories following a procedure described in the original patent.[1] The Ti content *x*, expressed in TiO_2 weight percent, has been found to be 1.0, 1.4, 2.0, and 3.0. In the following we shall refer to those samples as samples 2−5. For comparison also a Ti-free silicalite has been synthesized in the same conditions, hereafter labeled as sample 1. With one of the aims of this study being the correlation between intensities of some spectroscopic features of TS-1 with the fraction of Ti isomorphic inserted in the MFI framework, we have addressed great care in carefully selecting only samples where the insertion of Ti in the MFI framework was complete, within the experimental incertitude. Note that this synthesis achievement, for a $x = 3.0$ sample, is far for being trivial. The complete insertion of Ti atoms in the MFI framework

(52) Miecznikowski, A.; Hamuza, J. *Zeolites* **1987**, *7*, 249. de Man, A. J. M.; van Beest, B. W. H.; Leslie, M.; van Santen, R. A. *J. Phys. Chem.* **1990**, *94*, 2524.

(53) Yu, L.; Xiong, G.; Li, C.; Xiao, F.-S. *J. Catal.* **2000**, *194*, 487.

(54) (a) Nishimura, Y.; Hirakawa, A. Y.; Tsuboi, M. In *Advances in Infrared and Raman Spectroscopy*; Clark, R. J. H., Hester, R. E., Eds.; Heyden & Son: London, 1978. (b) Carey, P. R. *Biochemical Applications of Raman and Resonance Raman Spectroscopies*; Academic Press: New York, 1982 (and references cited therein).

has been proved by comparison of the amount of Ti determined by chemical analysis with the cell volumes obtained by Rietveld refinement of powder XRD data; see ref 11 for more details. Absence of extraframework TiO_2 particles has been proven by UV−vis and XANES spectroscopies (vide infra) and by the absence of the 144 cm^{-1} Raman band (spectra not reported for brevity). In fact, the 144 cm^{-1} band, very strong in Raman spectra of TiO_2, has been used for more than 10 years to detect even small traces of extraframework Ti in titanosilicates,[19,55,56] and thus to distinguish between high- and low-quality TS-1 samples.

For IR spectra a Brucker IFS 66 FTIR spectrometer equipped with an HgCdTe cryodetector has been used. For all spectra a resolution of 2 cm^{-1} has been adopted. Samples have been studied in transmission mode on thin self-supported wafers. Adsorbates have been dosed in gas phase through a vacuum manifold directly connected with the measure cell.

The conventional Raman spectra were obtained on a Perkin-Elmer 2000 near-IR−FT Raman spectrometer equipped with an InGaAs detector. The lasing medium was an Nd:YAG crystal pumped by a high-pressure krypton lamp, resulting in an excitation wavelength of 1064 nm (9398 cm^{-1}). The power output was ca. 1000 mW. Samples were examined as such or contacted with solutions.

UV resonance Raman spectra were obtained using a Renishaw Raman System 1000 by exciting with a frequency doubled Ar^+ laser, operating at 244 nm (40 984 cm^{-1}). The photons scattered by the sample where dispersed by a 3600 lines/mm grating monochromator and simultaneously collected on a UV-enhanced CCD camera. The collection optic was a •40 objective. A laser output of 12 mW was used, which resulted in a maximum incident power at the sample of approximately 2 mW. An exposure time of 240 s/spectrum was used.

XANES spectra have been collected, at room temperature on samples activated at 120 °C, at the GILDA MB8 beamline[57] at the European Synchrotron Radiation Facility (ESRF) in Grenoble. The monochromator was equipped with two Si(311) crystals, while harmonic rejection was achieved using mirrors. To ensure very high quality XANES spectra, the geometry of the beam line was optimized to improve the energy resolution (actual energy resolution better than 0.3 eV). A sampling step of 0.1 eV has been adopted. Four successive XANES spectra have been collected for each TS-1 sample; this procedure allow us to give, for the preedge peak intensity, a mean value and a corresponding standard deviation. EXAFS spectra have been collected at the EXAFS13 beam line of the DCI storage ring of the LURE facility in Orsay according to the experimental procedure described in detail elsewhere.[29]

3. Computational Methods

3.1. Cluster Models. Geometry optimization and vibrational frequency calculation of cluster models were performed both with the Hartree−Fock (HF) and density functional methods using the B3LYP functional. According to Sauer and deMan,[40] the cluster geometry was fixed to have S_4 symmetry. The basis set adopted is the standard 6-31G(d) in all cases.[58] The program used was Gaussian98.[59] Because our HF frequencies are in good agreement with the B3LYP ones when scaled in the usual way (scale factor 0.9), in the following we will discuss only the unscaled B3LYP results. In models containing several dangling OH groups, the SiOH bending vibrations were strongly coupled with the Si−O and Ti−O stretching modes. To simplify the analysis of the latter, in some cases we substituted ^1H with ^3H in OH groups in order to decouple their bending vibrations. This led to only small shifts of the Si−O and Ti−O vibrations (2−5 cm^{-1} was typical).

3.2. Embedded Cluster Models. Embedded cluster calculations were performed with the QMPOT method,[60] coupling a quantum mechanical description of a core set of atoms with a molecular mechanics description of the periodic solid. The QM cluster was treated at the Hartree−Fock level with a split valence SVP basis set.[61] The periodic solid was described with a shell model potential parametrized on QM calculations using the same level of theory.[47] The choice of different methods and basis sets for the cluster and embedded cluster calculations was dictated by the availability of the force field for Ti−O interactions. The programs used for the calculation of the subsystems were Gaussian98[59] and GULP,[62] InsightII[63] was the graphical interface program. Periodic vibrational frequencies were calculated for $k = 0$ (858 modes) and converted into an approximate density of states by assigning a Gaussian shape with constant width (10 cm^{-1}) and area to each mode, and summing over all modes.

4. Results and Discussion

This section is organized as follows. First, we will present the result of a series of new experiments adopting the traditional diagnostic techniques used to determine the amount of tetrahedral titanium in catalysts. These data form quantitative evidence of the correlation of the intensity of the IR band at 960 cm^{-1} with Ti content.

Subsequently, we will present our own verification of some recent resonant Raman experiments,[22] together with new accurate (normal) Raman experiments on the same samples. These results confirm the presence of several Ti-related spectroscopic features, whose intensity is variably affected by UV resonance. Then, we interpret the observed vibrations by comparison with the vibrational structure of large clusters and a periodic model, calculated with ab initio quantum chemical methods.

Finally, we report on the modification of the Ti-related spectroscopic features upon distortion of the tetrahedral symmetry of Ti caused by water absorption, underlining the relevance of symmetry in determining the enhancement selection rules of Raman spectroscopy.

4.1. IR Spectra of TS-1: Quantitative Evidence of the Correlation of the 960 cm^{-1} Band with Ti Content. Even if the 960 cm^{-1} band is generally recognized as a proof that Ti(IV) heteroatoms are isomorphically inserted in the zeolite structure,[1,14−21,24] a quantitative correlation between the Ti content (x) and the intensity of the 960 cm^{-1} IR band is still lacking because of the experimental difficulties related to its great intensity at high Ti content and because its frequency and intensity are modified by adsorbed molecules. For this reason, great care has been taken to prepare TS-1 pellets as thin as possible and to measure TS-1 samples that have undergone the same dehydration treatment.

Figure 1a reports the IR spectra of four TS-1 samples containing increasing Ti content (x) (curves 2−5) compared with pure silicalite (curve 1). The intensities of the spectra have been normalized on the overtone and combination crystal modes, i.e.

(55) Astorino, A.; Peri, J. B.; Willey, R. J.; Busca, G. *J. Catal.* **1995**, *157*, 482.
(56) Li, C.; Xiong, G.; Liu, J.; Ying, P.; Xin, Q.; Feng, Z. *J. Phys. Chem.* **2001**, *105*, 2993.
(57) Pascarelli, S.; Boscherini, F.; D'Acapito, F.; Meneghini, C.; Hrdy J.; Mobilio, S. *J. Synchrotron Radiat.* **1996**, *3*, 147.
(58) Petersson, G. A.; Bennett, A.; Tensfeldt, T. G.; Al-Laham, M. A.; Shirley, W. A.; Mantzaris, J. *J. Chem. Phys.* **1996**, *89*, 2193.
(59) Frisch, M. J.; Trucks, G. W.; Schlegel, H. B.; Scuseria, G. E.; Robb, M. A.; Cheeseman, J. R.; Zakrzewski, V. G.; Montgomery, J. A., Jr.; Stratmann, R. E.; Burant, J. C.; Dapprich, S.; Millam, J. M.; Daniels, A. D.; Kudin, K. N.; Strain, M. C.; Farkas, O.; Tomasi, J.; Barone, V.; Cossi, M.; Cammi, R.; Mennucci, B.; Pomelli, C.; Adamo, C.; Clifford, S.; Ochterski, J.; Petersson, G. A.; Ayala, P. Y.; Cui, Q.; Morokuma, K.; Malick, D. K.; Rabuck, A. D.; Raghavachari, K.; Foresman, J. B.; Cioslowski, J.; Ortiz, J. V.; Baboul, A. G.; Stefanov, B. B.; Liu, G.; Liashenko, A.; Piskorz, P.; Komaromi, I.; Gomperts, R.; Martin, R. L.; Fox, D. J.; Keith, T.; Al-Laham, M. A.; Peng, C. Y.; Nanayakkara, A.; Gonzalez, C.; Challacombe, M.; Gill, P. M. W.; Johnson, B.; Chen, W.; Wong, M. W.; Andres, J. L.; Gonzalez, C.; Head-Gordon, M.; Replogle, E. S.; Pople, J. A. *Gaussian 98*, Revision A.7; Gaussian, Inc.: Pittsburgh, PA, 1998.
(60) (a) Eichler, U.; Kölmel, C.; Sauer, J. *J. Comput. Chem.* **1997**, *18*, 463. (b) Eichler, U.; Brändle, M.; Sauer, J. *J. Phys. Chem. B* **1997**, *101*, 10035.
(61) Schäfer, A.; Horn, H.; Ahlrichs, R. *J. Chem. Phys.* **1992**, *97*, 2571.
(62) Gale, J. *J. Chem. Soc., Faraday Trans.* **1997**, *93*, 629.
(63) *InsightII 4.0.0 Molecular Modelling System*; Molecular Simulation Inc.: San Diego.

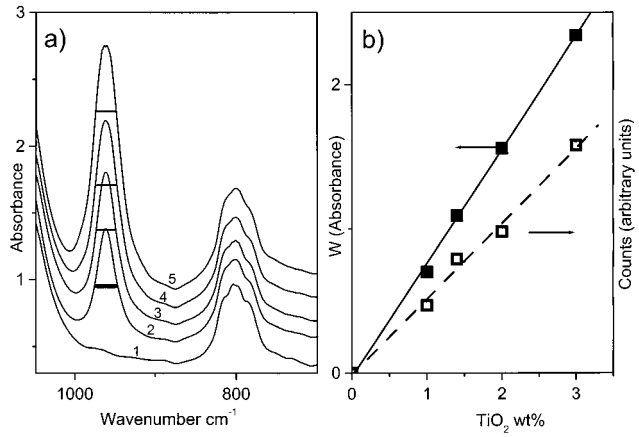

Figure 1. (a) IR spectra of outgassed thin pellets of silicalite (curve 1) and TS-1 with increasing Ti content x (curves 2−5). Spectra were normalized by means of the overtone bands between 1500 and 2000 cm^{-1} (not shown) and vertically shifted for the sake of clarity. The thick horizontal line represents the fwhm of the 960 cm^{-1} band for sample 2. By assuming that this band has a constant fwhm for any x, we obtain the absorbance W as the ordinate where the band as the same fwhm as in curve 2 (horizontal thin lines); see text. (b) Intensity W of the 960 cm^{-1} IR band (normalized absorbance units) as a function of x (full squares) and corresponding Raman counts (open squares); see section 4.2.

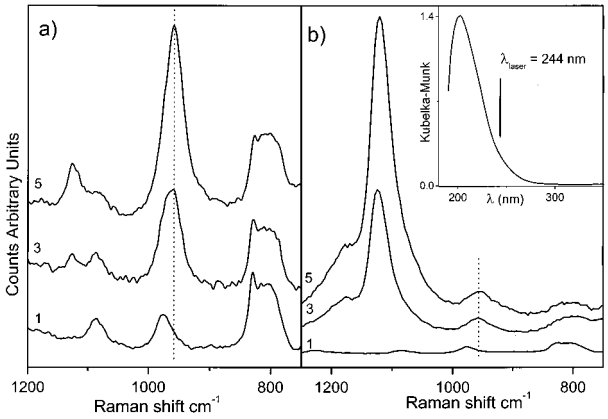

Figure 2. Raman spectra of samples 1 (silicalite), 3, and 5 (TS-1). (a) Spectra collected with a $\lambda = 1064$ nm (9398 cm^{-1}) excitation. (b) Spectra collected with a $\lambda = 244$ nm (40 984 cm^{-1}) excitation. Inset, UV−DRS spectrum of sample 5: vertical arrow indicates the excitation λ used for collecting the spectra reported in part b. Vertical dotted lines are placed at 960 cm^{-1}. Spectra of both parts have been vertically shifted for sake of clarity.

by assuming that the bands in the 1500−2000 cm^{-1} range are not affected by the presence of Ti and that their intensities are only a function of sample thickness (for the sake of simplicity this portion of the spectra is not reported). The quality of the normalization procedure is confirmed by the good superposition of the spectra in the 750−850 cm^{-1} range, which is also not influenced by Ti content.

The common method based on the dilution with KBr cannot be used for reducing the intensities of the framework modes, since it does not allow thermal treatments, needed in order to remove the adsorbed water, which would alter the frequency and intensity of the 960 cm^{-1} band[15,17] (vide infra section 4.5).

Therefore, we have used the following procedure in order to extract quantitative intensity data from all the spectra, also in the presence of nonlinear detector response due to saturation occurring for the maxima of the 960 cm^{-1} peaks measured on samples with high x. We assume that (i) the 960 cm^{-1} band does not saturate for the TS-1 sample with lowest Ti content and (ii) the ≪true≫ full width at half-maximum (fwhm) of this band is constant over all sets of TS-1 samples. The former assumption is supported by the fact that the intensity of the 960 cm^{-1} band, for the $x = 1.0$ sample, is less than 1.5 in absorbance units, while the latter is exactly what is expected for a band associated with different concentrations of a unique species. Assumption (i) allows us to measure the ≪true≫ fwhm of the 960 cm^{-1} band in TS-1 samples (27 cm^{-1}). Now, following assumption (ii), we were able to estimate for all samples reported in Figure 3, the absorbance (W) at the height where the width of the band corresponds to 27 cm^{-1}. This method minimizes the errors due to the instrument sensibility and allows a quantitative estimation of the band intensity. Such obtained values plotted against x in Figure 1b (■ data), give a high linear correlation ($r = 0.9998$) and validate assumptions (i) and (ii). Further validation comes from the similar linearity found for the intensities of the corresponding Raman band, which is not affected by saturation problems; see Figure 1b (□ data) and section 4.2.

Other experiments on defective silicalites and TS-1, containing variable amounts of hydroxyls,[13,17,51] confirm that Si−O vibrations in silanols exhibit a broad absorption in this region: however, they cannot be confused with framework Ti-sensitive modes because their intensity is very low, and the frequency is higher (975 vs 960 cm^{-1}).

4.2. Raman Spectra of TS-1: Evidence of the Correlation of the 1125 and 960 cm^{-1} Bands with Ti Content. Figure 2 reports the Raman spectra of two TS-1 samples with different Ti content and that of a silicalite sample with a high concentration of hydroxy defects. Part a of the figure reports spectra collected with a FTIR Raman spectrometer [$\lambda_{laser} = 1064$ nm (9398 cm^{-1})], while part b of the figure shows spectra obtained with a dispersive instrument working with a $\lambda_{laser} = 244$ nm (40 984 cm^{-1}). With the latter experimental setup we are in resonant Raman conditions for the $O^{2-}Ti^{4+} \rightarrow O-Ti^{3+}$ ligand to metal charge-transfer transition (LMCT).[64] In fact, for tetrahedral coordinated Ti^{4+} this LMCT exhibits an absorption band centered around 205 nm (about 49 000 cm^{-1}) with a low-energy tail extending down to 250 nm (40 000 cm^{-1});[19,23,24,29] see inset. The spectrum of the silicalite sample is very similar in both cases: in fact no resonant enhancement is expected for a sample transparent at that wavelength, the $O^{2-}Si^{4+} \rightarrow O^{-}Si^{3+}$ LMCT of [SiO_4] units occurring at much higher energies. Silicalite shows two bands at 1085, 975 cm^{-1} and a complex absorption centered at 820 cm^{-1}. The band at 1085 cm^{-1} has been associated with ν_{asym}(T−O−T) (Raman inactive),[17] while the stronger absorption at 975 cm^{-1} has been assigned to ν_{asym}-(T−O−T*), where T* is a T site where an hydroxy group is connected.[17] Even if this components lies in the same spectral region as the 960 cm^{-1} band, occurring with a $\Delta\nu = 15$ cm^{-1}, it can be easily distinguished; see vertical lines in Figure 2. Finally the complex absorption centered at 820 cm^{-1} has been associated with the ν_{sym}(T−O−T) (Raman active).[17] Moving now to TS-1 samples, we observe two main differences: (i) the appearance of a new band at 1125 cm^{-1}, visible in both type of experiments (see Figure 2), which is strongly enhanced by resonant Raman effect (see Figure 2b); (ii) the presence of a band at 960 cm^{-1}, growing with Ti content. Part b of Figure 1 reports, for the whole set of samples, the quantification of the latter statement: the linearity of the Raman data is less

(64) Please note that the ≪$O^{2-}Ti^{4+} \rightarrow O-Ti^{3+}$≫ nomenclature is only formal because this transition does not involve only one specific oxygen of the [TiO_4] unit but it should be considered as an absorbtion band of the whole tetrahedral species.

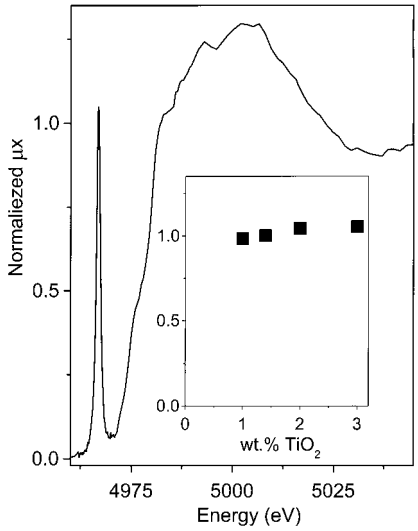

Figure 3. XANES spectrum of a typical TS-1 sample in a vacuum. Inset: intensity of the preedge peak (spectra normalized to the edge jump) for samples 2−5. Because the height of the edge jump is proportional to the Ti content, the intensity of the normalized preedge peak is invariant (within experimental incertitude) with Ti concentration.

spectacular than that obtained from IR data, reflecting the lower signal/noise ratio of Raman spectra. However, the interpretation of Raman data is straightforward, since they are not subjected to manipulations based on assumptions, such as those for the IR data. Moreover, for both resonant (Figure 2b) and nonresonant Raman spectra (Figure 2a), the constant value of the $I(1125)/I(960)$ ratio (0.25 and 11, respectively) suggests that the two bands should be related to two different spectroscopic manifestations of the same phenomenon (insertion of Ti in the MFI framework).

This set of UV−Raman data, where the increase of the 1125 cm^{-1} band intensity is correlated to the Ti content of different TS-1, agrees well with the experimental results of Li et al.,[56] showing a similar increase on the same sample along the crystallization process. Authors of ref 56 also report that the 960 cm^{-1} is only slightly changed by the crystallization process. This observation is used to conclude that the 960 cm^{-1} is not directly associated with the framework Ti−O−Si. We do not agree with this sharp conclusion since the much lower signal/noise ratio of the 960 cm^{-1} band (with respect to the Raman enhanced 1125 cm^{-1} one) in the spectra reported in Figure 5 of that work do not allow a straightforward conclusion. Moreover, at an intermediate crystallization stage, a nonquantified contribution of silanols in an amorphous phase (at 976 cm^{-1}) cannot be excluded. Finally, due to the high content of extraframework Ti species contained in the samples described in ref 56 (see broad low-energy tail in the UV DRS spectra, Figure 1, and the presence of the 144 cm^{-1} band in Raman spectra, Figure 2), a direct comparison with results obtained on high-quality TS-1 samples is hardly feasible.

4.3. XANES Data. The XANES spectrum of Ti(IV) in TS-1 is reported in Figure 3. The characteristic sharp preedge peak at 4967 eV has been ascribed to the Laporte allowed $A_1 \rightarrow E$ characteristic transition of tetrahedral [TiO_4] units.[24−26,28,30,33−35,65] This peak is due to the presence of Ti(IV) in tetrahedral coordination, and for this reason its intensity can be directly correlated with the amount of this species. In the past, the intensity of the preedge peak has been used to estimate the fraction of tetrahedral Ti(IV) by comparing the intensity of the preedge peaks of normalized spectra of some samples containing a different proportion between octahedral and tetrahedral Ti(IV).[66]

Even if the intensity of the 4967 eV preedge peak is proportional to the amount of framework Ti(IV) species, we are unable to directly correlate the intensity of this band in the raw X-ray absorption spectra with the Ti content (x) of the TS-1 sample, as was done for the 960 cm^{-1} band (see Figure 1). The reason for this lies in the fact that the X-ray absorption spectra around the Ti K-edge do not contain any feature ascribable to the hosting siliceous matrix, being both Si and O K-edges at much lower energies. So, we are unable to renormalize the raw X-ray absorption spectra to the sample thickness as we did for the IR spectra using the amplitude of the overtone crystal modes (vide supra section 4.1). For this reason normally XANES spectra are normalized to the edge jump, i.e. to the total amount of adsorbing atoms (Ti in our case) contained in the sample. The inset of Figure 3 reports the intensity of the 4967 eV preedge peak in the so normalized XANES spectra as a function of the Ti loading (x) of the different samples.

It is evident that the invariance[67] vs x of the intensity of the preedge peak in the XANES spectra normalized to the amount of Ti atoms (see inset of Figure 3) corresponds to the linear dependence observed for the intensity of 960 cm^{-1} band in the IR spectra normalized to the sample thickness (see Figure 1b). Given that the UV spectra show no presence of Ti other than tetrahedral (see inset in Figure 2b), the two correlations shown so far (of Ti content with XANES and IR features) can be coupled to demonstrate that the intensity of the 960 cm^{-1} IR peak in dehydrated samples is directly proportional to the concentration of *tetrahedral* Ti atoms.

4.4. Computational Models. 4.4.1. Cluster Model. Cluster models have been previously used to interpret the vibrational features of titanium silicates. In particular, Sauer and deMan[40] have calculated the vibrational spectra of a variety of small clusters, demonstrating that antisymmetric Ti−O−Si vibrations may appear at frequencies around 960 cm^{-1}. However, the occurrence and exact frequency of these vibrations vary widely with model size and connectivity, in a manner which has not yet been explained. The interpretation of the vibrational structure of cluster models containing open chains is much complicated by the strong coupling of the T−O stretching modes (where T is a generic tetrahedral atom) with the bending modes of terminal hydroxyls. This problem can be overcome by adopting clusters formed by closed rings: however, if small (e.g. four-membered) rings are adopted, the strain imposed by ring closure completely alters the vibrational features in the region of interest (700−1200 cm^{-1}), and the model is not representative. In this work, we focus on one type of cluster shown in Figure 4: a central tetrahedron surrounded by four complete tetrahedra, also known as the "shell-3" model because it contains three complete shells of neighbors of the central atom.

This choice is justified by the fact that, contrary to the original interpretation,[15,17,49] not only a single tetrahedron model cannot account for the gap between the 800 and 1100 cm^{-1} bands of silicates, but also models with several tetrahedra must possess

(65) Waychunas, G. A. *Am. Mineral.* **1987**, *72*, 89. Dingwell, D. B.; Paris, E.; Seifert, F.; Mottana, A.; Romano, C. *Phys. Chem. Miner.* **1994**, *21*, 501. Farges, F.; Brown, G. E., Jr.; Rehr, J. J. *Geochim. Cosmochim. Acta* **1996**, *60*, 3023.

(66) Trong On, D.; Kaliaguine, S.; Bonneviot, L. *J. Catal.* **1995**, *157*, 235.

(67) The small differences in the data reported in the inset of Figure 3, showing an intensity of the preedge peak moving from 0.98 ($x = 1$) to 1.05 ($x = 3$), are to be considered within the experimental incertitude of the technique.

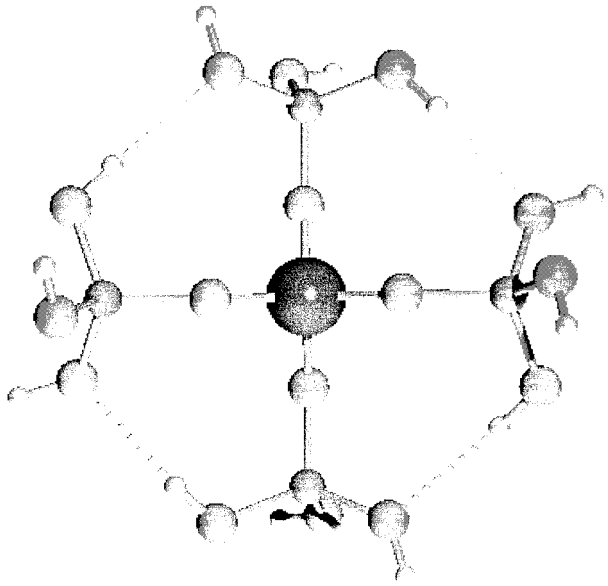

Figure 4. Cluster models. The central tetrahedral atom is Si or Ti (in SiSi4 and TiSi4, respectively).

at least one inner tetrahedron surrounded by four complete SiO_4 tetrahedra in order to show all the relevant vibrational features of the real material. We therefore avoid the discussion of the vibrations in terms of T_d symmetry, $\Gamma_{\text{stretching}} = T_2(\text{IR}) + A_1(\text{Raman})$, because the tetrahedral symmetry is lost after the first coordination shell.

This work refines the discussion of ref 40 in three directions. First, we have improved the accuracy of the calculations for the isolated cluster, by using density functional theory and the 6-31G(d) basis set. Second, we have simplified the interpretation of the results by using isotopic substitution (^{1}H substituted with ^{3}H) to reduce the coupling of Si−O−H bending modes with Si−O and Ti−O stretching modes. Finally, we have attempted the calculation of the vibrational spectrum of a true periodic model of TS-1, by embedding the above-mentioned cluster into a periodic lattice treated with interatomic potentials.

The vibrational modes of the $Si[OSi(OH)_3]_4$ and $Ti[OSi(OH)_3]_4$ models (named SiSi4 and TiSi4 in the following) can be analyzed either according to the symmetry of the vibration around the central T atom of each tetrahedron or according to the symmetry of the deformation of the single T−O−Si bridge. The latter deformation can occur either with symmetrical or antisymmetrical stretching of the two bonds. We can further separate the modes according to the symmetry of the deformation of the four T−O−Si bridges around the central T atom. An example is given in Figure 5. The symmetric and antisymmetric modes of a T−O−Si bridge are shown in part a. In part b the totally symmetric stretching mode of the inner tetrahedron is represented, which can also be seen as an in-phase combination of four T−O−Si antisymmetric modes or, if we neglect the central atom or consider it like a simple perturbation, like an in-phase stretching of the four neighboring Si−O oscillators. In part c of Figure 5, one of the asymmetric modes of the central tetrahedron is represented, which can also be described as an out-of-phase combination of the antisymmetric vibration of the four T−O−Si bridges or as an out-of-phase stretching of the four neighboring Si−O bonds. We will see later that these modes have different responses to the Si/Ti substitution. The main spectroscopic features of the SiSi4 and TiSi4 models are described in Figures 6 and 7 and Table 1, together with their assignment in terms of vibrations of TO_4 or T−O−Si units.

In the computed spectra of both of SiSi4 and TiSi4 clusters, the highest modes are represented by stretching modes of the central atom of the cluster. In the case of TiSi4, only one stretching of the central tetrahedron falls in this region, which is also an in-phase antisymmetric stretching of the four TiOSi bridges (1097 cm^{-1}); see Figure 7. Due to its symmetry around the Ti atom, this mode is the only candidate for the assignment of the 1125 cm^{-1} Raman band observed experimentally; see Introduction and vide supra section 4.2. It is completely IR-inactive due to its symmetry. The analogous mode for SiSi4 is observed at 1159 cm^{-1}. When the symmetric deformations of TO_4 involve symmetric T−O−Si stretching, due to the greater displaced mass, such modes appear at considerably lower frequencies: 827 and 814 cm^{-1} for SiSi4 and TiSi4, respectively (see Figures 6 and 7 and Table 1).

If we consider now the asymmetric stretching modes of the central tetrahedron (occupied by Ti or Si), the two models are much different. The asymmetric deformations of SiO_4 in SiSi4 produce features at 1105 and 1096 cm^{-1} when they occur through antisymmetric Si−O−Si stretching (see Figure 6 and Table 1). On the contrary, TiO_4 asymmetric vibrations in TiSi4 appear below 1000 cm^{-1}: a multiplet at 986, 968, 965, 909, and 897 cm^{-1} (see Figure 7 and Table 1). When the asymmetric deformations of TO_4 involve symmetric T−O−Si stretching, modes at 876, 855 cm^{-1} and at 829, 824 cm^{-1} occur for SiSi4 and TiSi4, respectively. This fact leads us to the discussion of the bands appearing in the central region of the spectra (850−1000 cm^{-1}), i.e. in the experimentally observed "gap" between the high-frequency (1250−1050 cm^{-1}) antisymmetric Si−O−Si vibrations and the low-frequency (around 800 cm^{-1}) symmetric Si−O−Si vibrations. This region is of much interest, because it contains (i) the highly debated 960 cm^{-1} band observed in both IR and Raman spectra and (ii) the features associated with framework defects.

The calculated spectrum of SiSi4 in this region contains only Si−O stretching modes associated with terminal Si−OH groups of the models. These modes are spread over a wide range (917−996 cm^{-1}; see Figure 6 and Table 1) because of the different hydrogen bonds involving the terminal OH groups of the cluster. These modes are good candidates for interpreting the IR modes appearing in the gap of defective silicates (e.g. defective silicalite).[17,49,51] No stretching modes of the central tetrahedron appear in this region. This is confirmed by our calculation on the periodic model (SiSi4 embedded in the periodic structure; vide infra Figure 9), which correctly reproduce the experimentally observed gap between 850 and 1000 cm^{-1}.

In the case of the TiSi4 cluster, the Si−OH stretching modes are strongly coupled with asymmetric TiO_4 stretching modes. These modes are out-of-phase combinations of the four Ti−O−Si antisymmetric stretching. They also span a wide frequency range (897−987 cm^{-1}), and no single mode can be associated individually with the 960 cm^{-1} band. This clearly shows, on one hand, that our cluster is inadequate for modeling a nondefective titanosilicate and, on the other hand, that in defective titanosilicates the Si−OH and asymmetric TiO_4 vibrations are strongly coupled. This is why spectroscopic features in this range are still under debate.[22,50]

4.4.2. Embedded Cluster Model. The previous discussion shows that the modeling of a nondefective titanosilicate requires either larger clusters or a periodic model. We have embedded the shell-3 clusters into the crystallographic T(5) position of a unit cell of the MFI framework (Figure 8). In the case of the embedding of the *SiSi4* cluster, the resulting structure is purely siliceous, while for the *TiSi4* cluster, we obtain a structure with

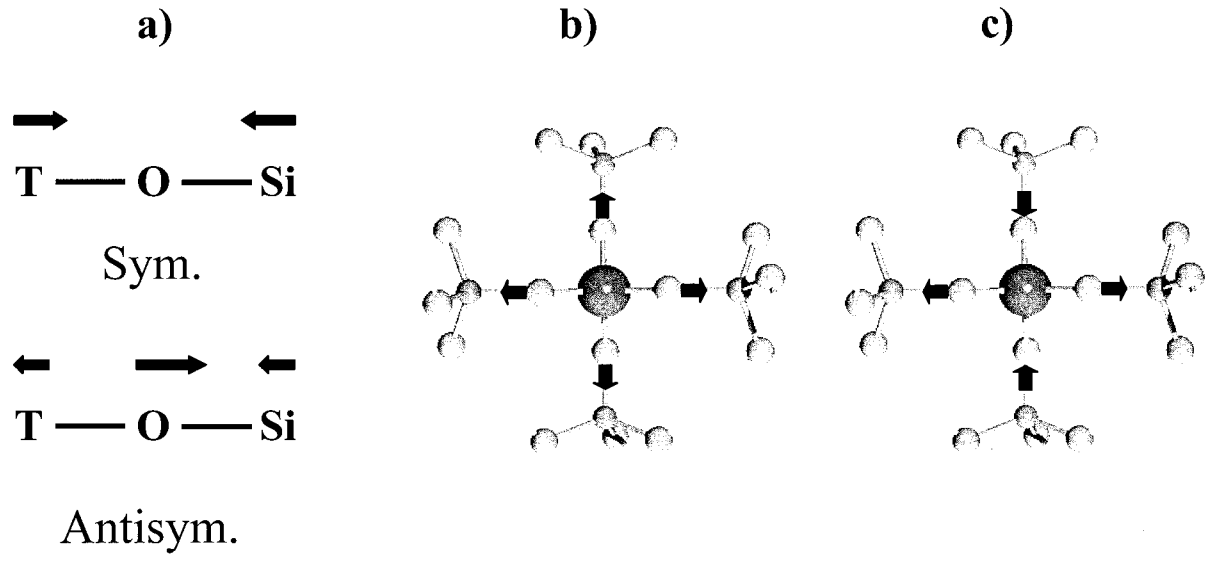

Figure 5. (a) Definition of "symmetric" and "antisymmetric" stretching of the T−O−T bridges. (b) Symmetric stretching of the central tetrahedron, achieved through in-phase antisymmetric stretching of the four connected T−O−Si bridges. (c) One of the asymmetric stretching modes of the central tetrahedron, achieved through out-of-phase antisymmetric stretching of the T−O−Si bridges.

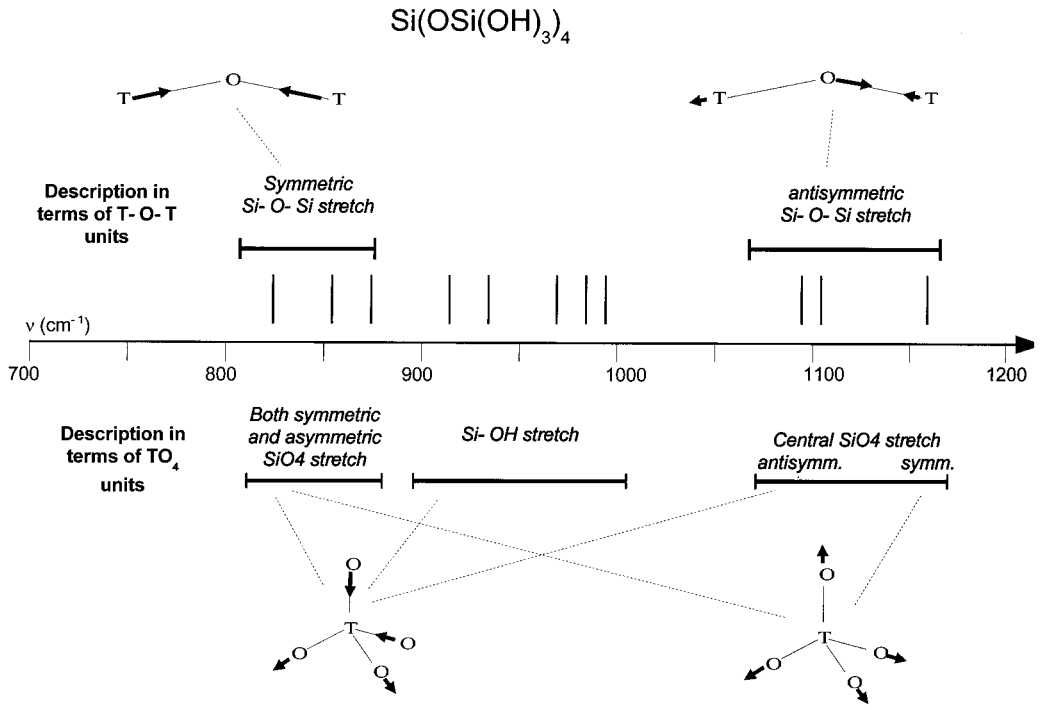

Figure 6. Calculated vibrational frequencies for the $Si[OSi(OH)_3]_4$ model, classified following the symmetries of the T−O−T unit (upper part) or according to the symmetries of the $[TO_4]$ unit (lower part).

one Ti atom per unit cell. No hydroxy groups are present in either model. The choice of the T(5) position is partly arbitrary and dictated by the availability of the optimized structure from a previous work.[47] Figure 9 reports the calculated density of states of silicalite and TS-1. The DOS of silicalite correctly reproduces the two main groups of framework vibrations together with the gap between them in the 850−1000 cm^{-1} region; see IR spectra reported in Figure 1. The DOS of titanium−silicalite is very similar but differs for a small, expected,[1,14,15,17,18,20,24] feature at 960 cm^{-1} (inset of Figure 9). Graphical analysis of the individual normal modes contributing to the DOS at this frequency shows four contributions: two modes involving antisymmetric stretching of Si−O−Si bridges far from the Ti atom and two modes which can be classified as out-of-phase asymmetric stretching of the Ti−O−Si bridges (Figure 5c). The former have no counterpart in cluster calculations and may be artifacts due to a faulty modeling of the interface between the QM and MM regions, while the latter are in full agreement with the cluster calculations and with the assignment of the 960 cm^{-1} band presented above. This result, although not conclusive due to the limitations of the model, indicates that the embedding of the TiSi4 cluster into a nondefective periodic framework causes the disappearance of the scattered (897−987 cm^{-1}) bands due to coupled Ti−O−Si−OH vibrations and the appearance of a single narrow band at 960 cm^{-1}.

Quantum mechanical calculations not only provides vibrational frequencies to be compared with the experimental ones

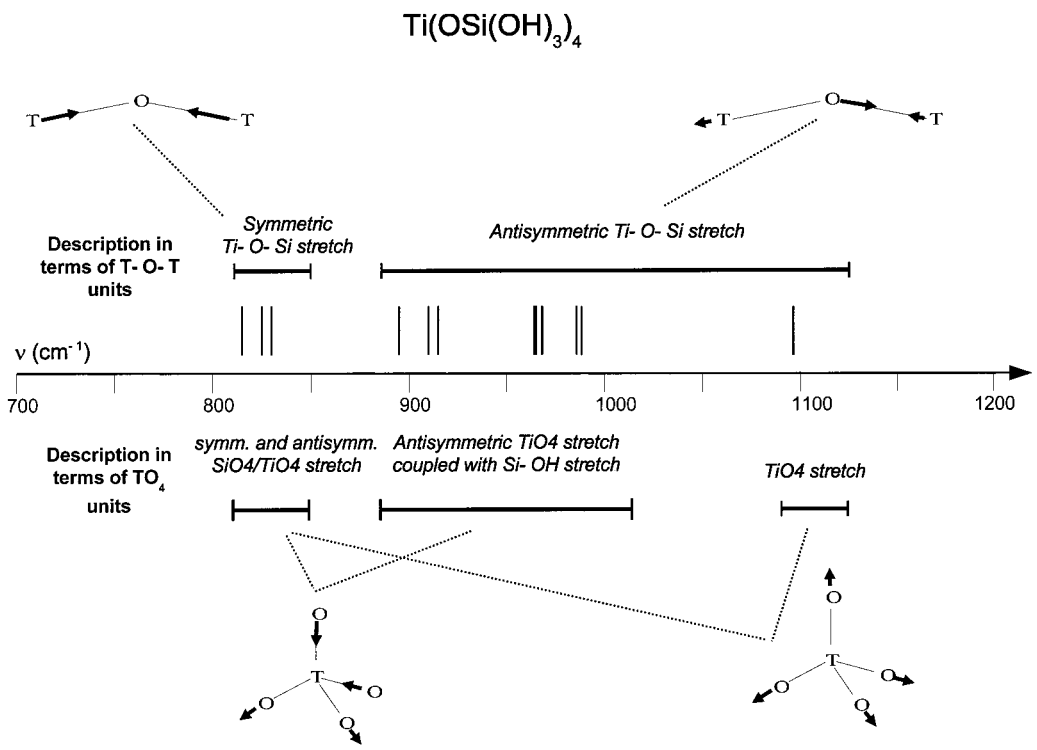

Figure 7. Same as Figure 6 for the calculated vibrational frequencies for the $Ti[OSi(OH)_3]_4$ model.

Table 1

(A) Computed Stretching Frequencies for the $Si[OSi(OH)_3]_4$ Model (ν) and Symmetry of the Corresponding Mode with Respect to the Central SiO_4 and Si−O−Si Unit[a]

ν (cm^{-1})	SiO_4	SiOSi	comments
1159	S	A	see text
1105, 1096	A	A	see text
996, 984, 971			SiO stretching modes of terminal silanols involved in hydrogen bonds with neighboring OH as donors
993			SiO stretching modes of terminal silanol (no H-bond)
917			SiO stretching modes of terminal silanol in which O is hydrogen bond acceptor
876, 855	A	S	see text
827	S	S	see text

(B) Same as A for the $Ti[OSi(OH)_3]_4$ Model and Symmetry of the Corresponding Mode with Respect to the Central TiO_4 and Ti−O−Si Units[a]

ν (cm^{-1})	TiO_4	TiOSi	comments
1097	S	A	see text
987, 964			SiO stretching modes of terminal silanols involved in hydrogen bonds with neighboring OH as donors
986, 968, 965, 909, 897	A	A	TiO stretching modes strongly coupled with SiO stretching modes of terminal silanols involved in H-bonds with neighboring OH as donors
913			SiO stretching modes of terminal silanols involved in hydrogen bonds with neighboring OH as acceptors
829, 824	A	S	see text
814	S	S	see text

[a] S = symmetric; A = asymmetric or antisymmetric for TiO_4 and Ti−O−Si units, respectively. Blank symmetry field corresponds to modes not involving the central tetrahedron.

but also describe the electronic structure of the clusters, which has deep implications in the resonant Raman experiments. In particular, the structure and symmetry of the LUMO of the Ti-containing clusters have to be considered (an accurate calculation of the true electronic structure of the excited state is beyond the scope of the present work). The LUMO of the TiSi4 cluster is almost totally symmetric around the Ti atom and 2-fold degenerate. The LUMO is formed by an antibonding combination of oxygen *p* orbitals with a totally symmetric combination of titanium *d* orbitals ($d(z^2)$, $d(x^2-y^2)$). The HOMO of the same cluster, on the contrary, is a combination of mainly nonbonding p orbitals on the four oxygen atoms surrounding titanium, with no contribution by the Ti orbitals.

These electronic features are in accordance with the attribution of the observed UV absorption at 205 nm (about 49 000 cm^{-1}) to a ligand to metal charge-transfer transition. This transition must involve a totally symmetric excited state in which all four Ti−O bonds are symmetrically stretched with respect to the ground state (due to the Ti−O antibonding character of the LUMO). Thus, the symmetric TiO_4 stretching at 1125 cm^{-1} meets both selection rules mentioned in the Introduction for the resonance enhancement of its Raman intensity: (a) it is

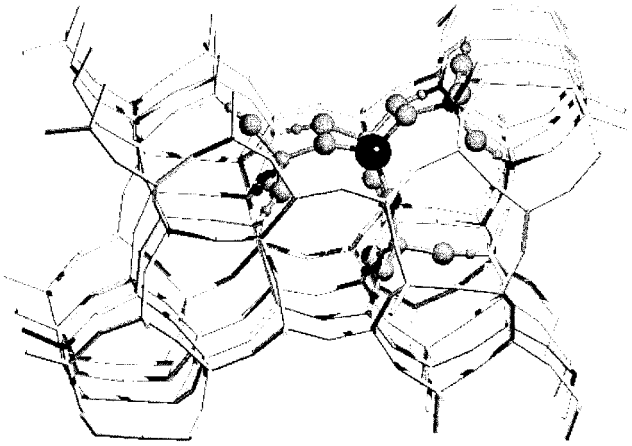

Figure 8. Representation of the embedded cluster models. Cluster models SiSi4 and TiSi4 are embedded into one of the T(5) crystallographic positions of the MFI framework. Periodic boundary conditions are then applied.

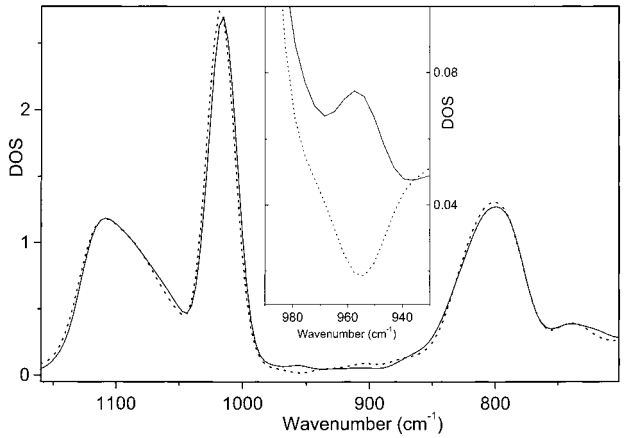

Figure 9. Calculated vibrational density of states for silicalite (dashed line) and TS-1 (solid line). The approximated DOS was calculated by assigning constant width (10 cm^{-1}) and intensity to each of the 858 ($k = 0$) modes. Inset: enlargement of the 960 cm^{-1} region.

totally symmetric with respect to the absorbing center, and (b) it causes the same molecular deformation induced by the electronic excitation. We therefore conclude that the observed band at 1125 cm^{-1} (calculated at 1097 cm^{-1} in the TiSi4 cluster; see Figure 7 and Table 1) can be attributed to this kind of vibration. On the basis of the discussion above, this vibration can be also described as the in-phase combination of the four Ti−O−Si stretching modes, or as the in-phase combination of the four $Si-O^{\delta-}$ bonds perturbed by the presence of $Ti^{\delta+}$.

On the contrary, none of the vibrations appearing in the "gap" meets either of the selection rules for Raman enhancement. This explains why the 960 cm^{-1} band is not enhanced. Indeed, it almost disappears in Resonant experiments due to the enormous intensity of the strongly enhanced 1125 cm^{-1} band. Nevertheless, the Ti-sensitive nature of the 960 cm^{-1} band is confirmed by nonresonant experiments, as discussed in the previous sections.

4.5. Perturbation of the Tetrahedral Ti(IV) Fingerprints of TS-1 upon Insertion of H_2O Molecules in Its First Two Coordination Shells: The Disappearance of the Enhancement for the 1125 cm^{-1} Band in UV−Raman Spectra. For more than 10 years,[14,15,17,24,28,33−35] the interaction of probe molecules with Ti(IV) centers in TS-1 has been used to prove the isomorphic insertion of Ti in the framework and to measure the modification induced on the different spectroscopic features

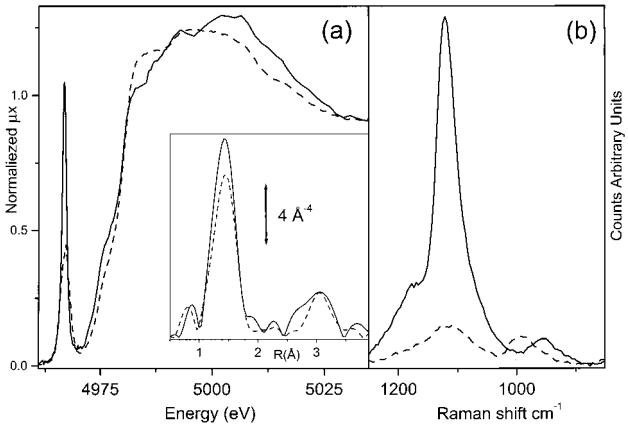

Figure 10. Effect of soaking TS-1 (sample 5) with water on the XANES and UV−Raman spectra parts a and b, respectively: dried TS-1 (full line); soaked TS-1 (dotted line). The inset in part a reports the k^3-weighted, phase uncorrected, Fourier transform of the corresponding EXAFS spectra.

of TS-1 by the distortion of the local geometry around Ti. In the late 1980s,[15] the progressive blue shift undergone by the 960 cm^{-1} band upon increasing the equilibrium pressure of H_2O, NH_3, and CH_3OH has been considered the definitive proof that the 960 cm^{-1} band could not be ascribed to Ti═O species; otherwise, a red shift would be expected upon interaction with probe molecules. In that work the first intuitive attribution of the 960 cm^{-1} band in terms of a Si−O vibration perturbed by an adjacent framework Ti center was reported. Only recently it has been demonstrated, using UV−Raman spectroscopy, that also the 1125 cm^{-1} band is sensitive to the local environment around the Ti species, being observed at 1085 cm^{-1} on Ti−SiO_2 prepared by chemical grafting[68] and at 1110 cm^{-1} in Ti−MCM-41.[69]

In this section, it is our aim to demonstrate that the proximity of the UV-absorbing (Ti) and vibrating groups is only a necessary condition, but not a sufficient one, for Raman enhancement. We have employed again the comparison between dried and soaked TS-1 (sample 5) as monitored by X-ray absorption and resonant Raman spectroscopies (Figure 10). The XANES spectra report a relevant decrease and broadening of the 4967 eV preedge peak, reflecting the distortion from the original tetrahedral symmetry around Ti(IV)[24−26,28,30,33−35,65,66] upon water absorption. The inset in part a reports the k^3-weighted, phase uncorrected, Fourier transform of the corresponding EXAFS spectra, demonstrating that water insertion modifies both the first and the second coordination shells around Ti(IV). Figure 10b shows that, beside a frequency shift of the 960 cm^{-1} band (now at 990 cm^{-1}) and a broadening of the 1125 cm^{-1} band (modifications already observed with non resonant Raman[17]), water absorption results in a strong extinction of the enhancement of the 1125 cm^{-1} band observed by using an UV−Raman source, which intensity has been reduced by a factor higher than 8. The total reversibility of the absorption of H_2O on TS-1 has been proved by the complete restoration of the EXAFS, XANES, Raman, and IR spectra upon sample activation at room temperature (not reported for brevity).

The "enhancement extinction" proves that the 1125 cm^{-1} band, which is recognized to be a Ti related vibration by all the authors who have faced this topic,[17,18,22,56] does no more

(68) Yang, Q.; Wang, S.; Lu, J.; Xiong, G.; Feng, Z.; Xin, Q.; Li C. *Appl. Catal. A* **2000**, *194−195*, 507.

(69) Yu, J.; Feng, Z.; Xu, L.; Li, M.; Xin, Q.; Liu, Z.; Li, C. *Chem. Mater.* **2001**, *13*, 994.

fulfill the two requirements for Raman enhancement: (a) total symmetry of the vibrations with respect to the absorbing center and (b) same molecular deformation induced by the electronic and vibrational excitations.[54] In fact, in the presence of coordinated water molecules, rule a is surely violated, while we cannot draw a priori conclusions on rule b, for which an *ad hoc ab initio* study would be required.

Coming to the shifts, while the blue shift of 30 cm^{-1} undergone by the 960 cm^{-1} band is evident, a quantitative determination of the shift undergone by the 1125 cm^{-1} band is not straightforward. In fact other Raman features are present in the 1050−1200 cm^{-1} interval: once the resonant effect is quenched, the intensity of the perturbed 1125 cm^{-1} band becomes comparable to that of the other features, resulting in an overall broad absorption. Quantitative location of the perturbed band is thus not feasible, and only a tentative location in the 1105−1115 cm^{-1} range can be guessed.

As a conclusion of this section, given the importance of symmetry of the Ti center in Raman enhancement, the absence of enhancement of the 960 cm^{-1} band cannot be used to support the thesis that this band is not related to Ti insertion in the MFI framework. Our attribution of the 960 cm^{-1} band (see section 4.4), on the contrary, does not predict any enhancement, because both rules a and b are violated.

5. Conclusions

This work gives a unified description of the vibrational features associated with the insertion of tetrahedral titanium in the MFI zeolite lattice and, more generally, in tetrahedral silicate frameworks. This description forms the base for the technical charachterization of Ti-containing silicate catalysts using spectroscopic methods, which is of capital importance in industrial catalysis. A combination of spectroscopic and computational techniques is used in order to assign the main vibrational features of TS-1, also taking into account the presence of hydoxylated defects.

A set of experiments on TS-1 samples with variable Ti content, synthesized and treated in an homogeneous and reproducible way, has allowed proof of the quantitative correlation between Ti content and the intensity of the 960 cm^{-1} IR and Raman feature. Combined IR and XANES experiments demonstrate that the 960 cm^{-1} feature is quantitatively associated with the presence of Ti in tetrahedral coordination.

Raman experiments on silicalite and TS-1 with excitation wavelengths of 1064 nm (nonresonant) and 244 nm (resonant) show that (a) the main features associated with Ti insertion in the lattice are vibrations at 1125 and 960 cm^{-1} (both are evident in both kinds of experiment, but the 1125 cm^{-1} is drastically enhanced by UV resonance, while the 960 cm^{-1} is not) and (b) a mode is observed at 978 cm^{-1} on defective silicalites attributed to the Si−O stretching in silanols. Even if occurring in the same spectral region, the 960 and 978 cm^{-1} bands cannot be confused because of their differences in frequency, shape, fwhm, and dependence upon Ti loading. Finally, we demonstrate, for the first time, that the distortion of the tetrahedral symmetry around Ti caused by water adsorption causes the extinction of the enhancement of the 1125 cm^{-1} band in UV−Raman spectra. This whole set of experiments confirms the first Raman enhanced spectrum of TS-1 reported in ref 22 and gives more complete interpretation of the vibrational features of TS-1.

Quantum mechanical calculations of the vibrational frequencies and the electronic structure of shell-3 cluster models allow assignment of the main vibrational features. The 1125 cm^{-1} peak is undoubtedly assigned to the symmetric stretching vibration of the TiO_4 tetrahedron, achieved through in-phase antisymmetric stretching of the four connected Ti−O−Si oscillators. According to its symmetry and to the electronic structure of the Ti moiety, this is the only vibration fulfilling the resonant Raman selection rules. This assignment is equivalent to the assignment to the in-phase stretching of the four Si−O bonds surrounding Ti. The asymmetric vibrations of TO_4 of our cluster models appear above 1000 cm^{-1} for T = Si and between 913 and 986 cm^{-1} for T = Ti. Cluster calculations show that in pure siliceous clusters no modes of the central SiO_4 tetrahedron occur in the 900−1000 cm^{-1} gap. On the contrary, upon Ti substitution some modes appear in this region although their frequencies are scattered (in the 897−986 cm^{-1} range) by the coupling with the modes of the external hydroxylated SiO_4. Finally embedding in the periodic structure removes this coupling, and the 960 cm^{-1} band is obtained. On the basis of these results, we confirm the assignment of the 960 cm^{-1} band to the asymmetric stretching of the TiO_4 unit, which can equivalently be described as the out-of-phase antisymmetric stretching of the four connected Ti−O−Si oscillators, or as the out-of-phase stretching of the four Si−O bonds pointing toward Ti.

Acknowledgment. This study has been supported by MURST COFIN2000 "*Structure and reactivity of catalytic centers in zeolitic materials*". We acknowledge the Renishaw for the kindly access to the UV−Raman instrument (R. Tagliapietra) and for scientific and technical support during measurements. We thank the BM8 GILDA staff at the ESRF and the EXAFS13 group of LURE (in particular F. D'Acapito and F. Villain) for the important scientific and technical support during X-ray absorption measurements. We are indebted to M. Ricci (EniChem Novara) for fruitful discussions.

Note Added in Proof. Very recently Soult et al.[70] have improved previous photoluminescence studies[29] on TS-1 by performing 12 K measurements. They have highlighted in the 490 nm emission (unambiguously attributed to titanium[29,70]) a resolved vibrational structure of 966 ± 24 cm^{-1}. This is a further important proof that the 960 cm^{-1} mode of TS-1 is directly related to the insertion of Ti in the zeolitic lattice.

JA010607V

(70) Soult, A. S.; Pooré, D. D.; Mayo, E. I.; Stiegman, A. E. *J. Phys. Chem. B* **2001**, *105*, 2687.